VARIATIONS IN THE SOYA WARM CURRENT OBSERVED BY HF OCEAN RADAR, COASTAL TIDE GAUGES AND SATELLITE ALTIMETRY

Naoto Ebuchi, Yasushi Fukamachi, Kay I. Ohshima, Kunio Shirasawa, Masaaki Wakatsuchi

Institute of Low Temperature Science, Hokkaido University, ebuchi@lowtem.hokudai.ac.jp

ABSTRACT: Three HF ocean radar stations were installed at the Soya/La Perouse Strait in the Sea of Okhotsk in order to monitor the Soya Warm Current. The frequency of the HF radar is 13.9 MHz, and the range and azimuth resolutions are 3 km and 5°, respectively. The radar covers a range of approximately 70 km from the coast. It is shown that the HF radars clearly capture seasonal and short-term variations of the Soya Warm Current. The velocity of the Soya Warm Current reaches its maximum, approximately 1 m s^{-1}, in summer, and weakens in winter. The velocity core is located 20 to 30 km from the coast, and its width is approximately 50 km. The surface transport by the Soya Warm Current shows a significant correlation with the sea level difference along the strait, as derived from coastal tide gauge records. The cross-current sea level difference, which is estimated from the sea level anomalies observed by the Jason-1 altimeter and a coastal tide gauge, also exhibits variation in concert with the surface transport and along-current sea level difference.

KEY WORDS: HF radar, Satellite altimetry, Soya Warm Current, Sea of Okhotsk, Coastal currents

1. INTRODUCTION

The Sea of Okhotsk (Fig. 1), a marginal sea adjacent to the North Pacific, is one of the southernmost seasonal sea ice zones in the Northern Hemisphere and it has been conjectured that it is a region in which the North Pacific Intermediate Water is ventilated to the atmosphere. The Sea of Okhotsk is connected with the Sea of Japan through the Soya/La Perouse Strait, which is located between Hokkaido, Japan, and Sakhalin, Russia. The Soya Warm Current (SWC) enters the Sea of Okhotsk from the Sea of Japan through the Soya Strait and flows along the coast of Hokkaido as a coastal boundary current. It supplies warm, saline water in the Sea of Japan to the Sea of Okhotsk. The current is roughly barotropic and shows a clear seasonal variation (Aota, 1984; Matsuyama et al., 1999). However, the SWC has never been continuously monitored due to the difficulties involved in field observations related to various reasons, such as severe weather conditions in winter, political issues at the border strait, and conflicts with fishing activities in the strait. Detailed features of the SWC and its variations have not been clarified. Information concerning the variations of the SWC and the water exchange between the Sea of Japan and the Sea of Okhotsk is important for the study of both of these seas. In the present study, variations of the SWC is investigated by combining the surface current fields observed by HF ocean radars with the sea level observations from coastal tide gauges and satellite altimetry.

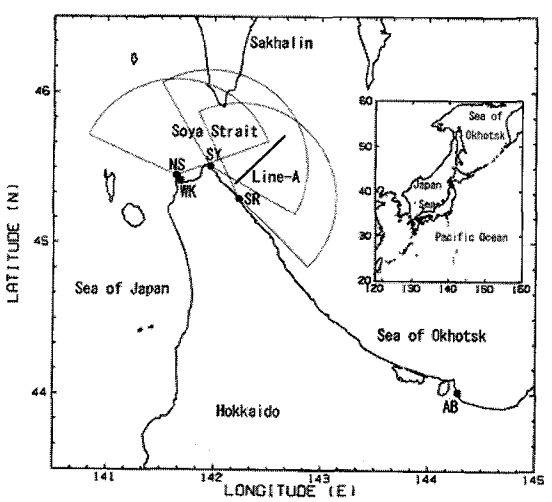

Figure 1. Map of the Soya/La Perouse Strait, and location and coverage of the HF radar stations.

2. OBSERVATION OF THE SWC USING HF RADARS

In order to continuously monitor the SWC, three HF radars (CODAR Ocean Sensors, SeaSonde, Barrick et al., 1977) were installed around the Soya Strait (Fig. 1). The frequency of the HF radar is 13.9 MHz, and the range and azimuth resolutions are 3 km and 5°, respectively. The HF radar covers a range of approximately 70 km from the coast. The observations have been made at one-hourly intervals. We measured the beam pattern of the receiving antenna and corrected for distortion of the antenna pattern to derive accurate radial velocities. Surface current vectors were composed in grid cells of 3 x 3 km using the radial velocity components observed by the radars according to a least squares method. This study analyzes data obtained over a period of 35 months, from August 2003 to June 2006.

An example of the observed surface current vector field is shown in Fig. 2. Figure 3 is an example of monthly-

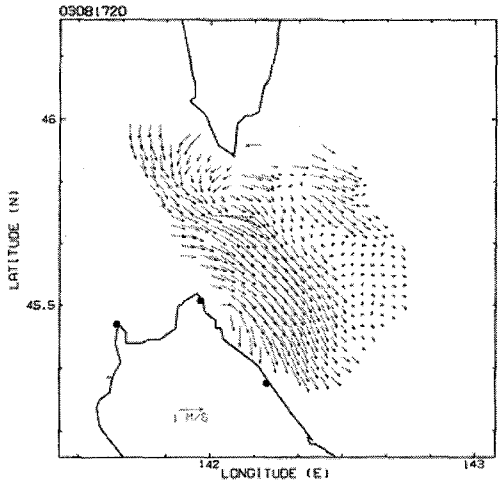

Figure 2. An example of hourly surface current vector field (1100 UTC, 17 August 2003).

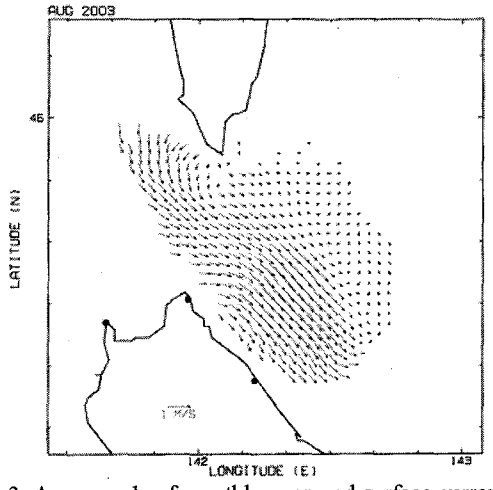

Figure 3. An example of monthly-averaged surface current field (August 2003).

averaged surface current field. In these figures, the SWC, which flows from west to east across the Soya Strait and turns toward southeast along the coast, is captured very clearly. They also show southward currents along the west coast of Sakhalin, as predicted by numerical experiments (Ohshima and Wakatsuchi, 1990; Ohshima, 1994).

The surface current velocity observed hourly by the HF radars was compared with in-situ data from drifting buoys and shipboard Acoustic Doppler Current Profilers (ADCPs) (Ebuchi et al., 2004; 2006a; 2006b). The current velocity derived from the HF radars showed good agreement with that observed using the drifting buoys (Fig. 4). The root-mean-square (rms) differences were found to be less than 25 cm s^{-1} for the zonal and meridional components. The observed current velocity was also found to exhibit reasonable agreement with the shipboard ADCP data (Ebuchi et al., 2004; 2006a; 2006b).

3. SEASONAL VARIATION OF THE SWC

Using the surface current vector fields observed by the HF radars, we discuss seasonal variations of the SWC. In order to remove the tidal constituents, a 25-hour running average was applied to the time series of the hourly surface current vectors in each grid cell, and then daily and monthly mean current fields were calculated. An example of the monthly-averaged field is shown in Fig. 3.

Daily southeastward current components across Line-A (Fig. 1) were averaged monthly and are shown with standard deviations in Fig. 5 for a period from August 2003 to July 2004. Figure 6 shows year-to-year variations of the monthly mean profiles within the three years from 2003 to 2006. The monthly-mean profiles show a clear seasonal variation. The velocity of the SWC reaches its maximum of approximately 1 m s^{-1}, in summer (August and September), and becomes weak in winter (January and February). The current axis is located 20 to 30 km from the coast in this region, and the typical width of the SWC is approximately 50 km. These features of the SWC are consistent with the results of short-term or point-wise observations reported in previous studies (Aota, 1984; Matsuyama et al., 1999).

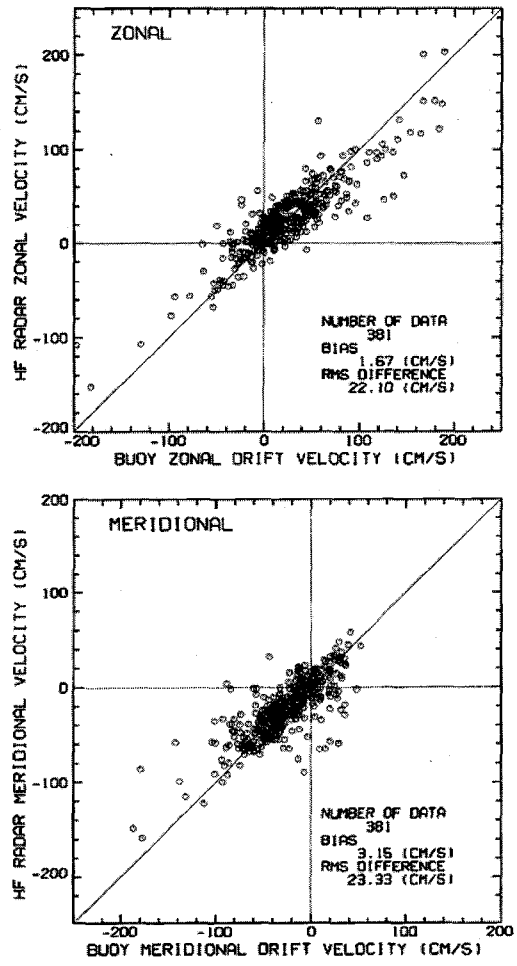

Figure 4. Comparison of HF radar with drifting buoy observations for zonal (upper) and meridional (lower) velocity components.

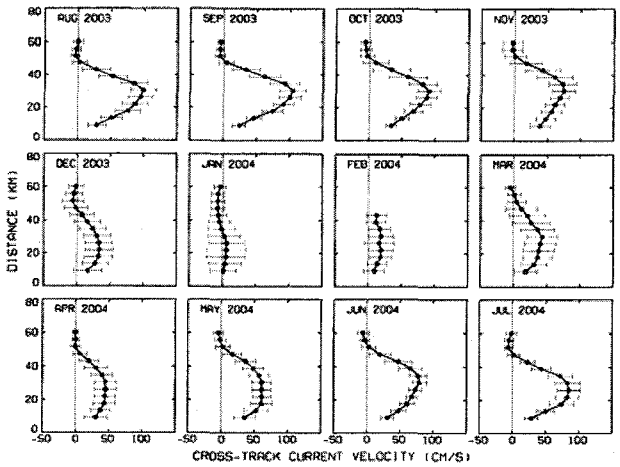

Figure 5. Monthly-averaged profiles of the southeastward current velocity component across Line-A (Fig. 1) with respect to the distance from the coast line for a period from August 2003 to July 2004.

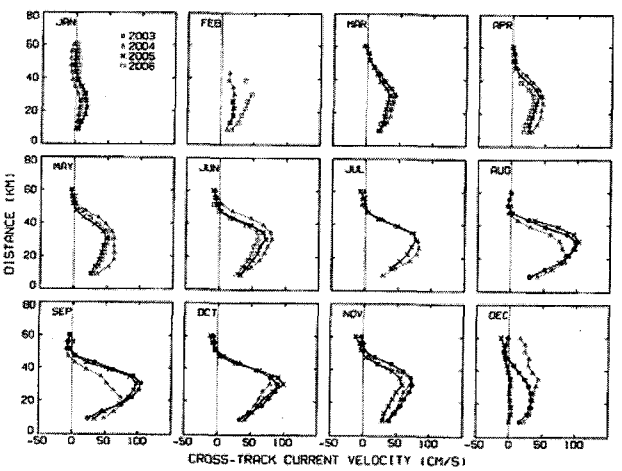

Figure 6. Year-to-year variations of the monthly-averaged profiles of the southeastward current velocity component across Line-A (Fig. 1).

4. VARIATIONS OF SURFACE TRANSPORT AND THEIR RELATIONSHIP WITH THE SEA LEVEL DIFFERENCES

Daily surface transport across Line-A (Fig. 1) was defined by the integration of the daily southeastward current component along the line from the coast to a point at which the component becomes negative. Figure 7 shows the time series of the surface transport (thick line). Note that the unit of surface transport is not volume/time but area/time, because the HF radars provide only the surface current velocity. Assuming a barotropic flow structure, if the surface transport is multiplied by a depth of 30 to 50 m, the maximum volume transport is roughly estimated to range up to 1 to 2 x 10^6 m^3 s^{-1} (or 1 to 2 Sv). In winter (from January to March), there often exists lack of data, because the observation region is covered by sea ice. Fukamachi et al. (2006) try to estimate the SWC volume transport by combining the HF radar data with vertical velocity profiles observed by bottom-mounted ADCP.

The driving force of the SWC is ascribed to the sea level difference between the Sea of Japan and the Sea of Okhotsk (Aota, 1984; Ohshima, 1994). The surface velocity of the SWC has been reported to be closely related to the sea level difference (Aota, 1984; Matsuyama et al., 1999). For comparison with the surface transport as observed by the HF radars, we calculated the sea level difference between two tide gauge stations, Wakkanai (labeled as WK in Fig. 1) and Abashiri (AB in Fig. 1), which represents sea level difference between the Sea of Japan and the Sea of Okhotsk. A 48-hour tide-killer filter was applied to the hourly tide gauge records at these stations. The daily-mean sea levels were then calculated, and atmospheric pressure correction was performed using the daily-mean sea level pressure observed at weather stations in the cities of Wakkanai and Abashiri. The time series is shown by a thin line in Fig. 7. The surface transport of the SWC and the sea level difference along the current show a good correlation with a correlation coefficient of 0.702. Both time series exhibit not only the seasonal variation but also variations with time scales of approximately 10 to 15 days. The results shown in Fig. 7 confirm the correlation at various time scales between the SWC and the along-current sea level difference.

In order to assess variations of the sea level difference in the cross-current direction, we utilized the sea level anomalies observed by the Jason-1 satellite altimeter. Figure 8 shows locations of ground tracks of Jason-1 in the Sea of Okhotsk. Since the spaceborne radar altimeter is not able to observe the sea surface height accurately in the region close to the coastline, we cannot obtain the cross-current sea surface height profiles associated with the SWC directly from the altimeter data. Therefore the difference of the sea level anomalies between the offshore observations by the altimeter (indicated by B in Fig. 8) and the coastal tide gauge records at the Wakkanai station is utilized to represent the sea level variations across the SWC.

In Fig. 7, the variation of sea level difference across the SWC is indicated by solid circles. The amplitude of the cross-current sea level difference is multiplied by 0.6 and is shifted vertically to match with the along-current sea level difference (thin line) in Fig. 7. The temporal interval of the Jason-1 observation is 9.91 days. It is shown that the cross-current sea level difference is well correlated with the along-current sea level difference and also with the surface transport of the SWC. These results support that the SWC is in the geostrophic balance in the cross-current direction, and is driven by the sea level difference between the Sea of Japan and the Sea of Okhotsk (Aota, 1984). The same relationship between the cross- and along-current sea level differences were discernible in the 10-year record of the sea level anomaly obtained by the TOPEX/POSEIDON altimeter combined with the coastal tide gauge records (not shown here).

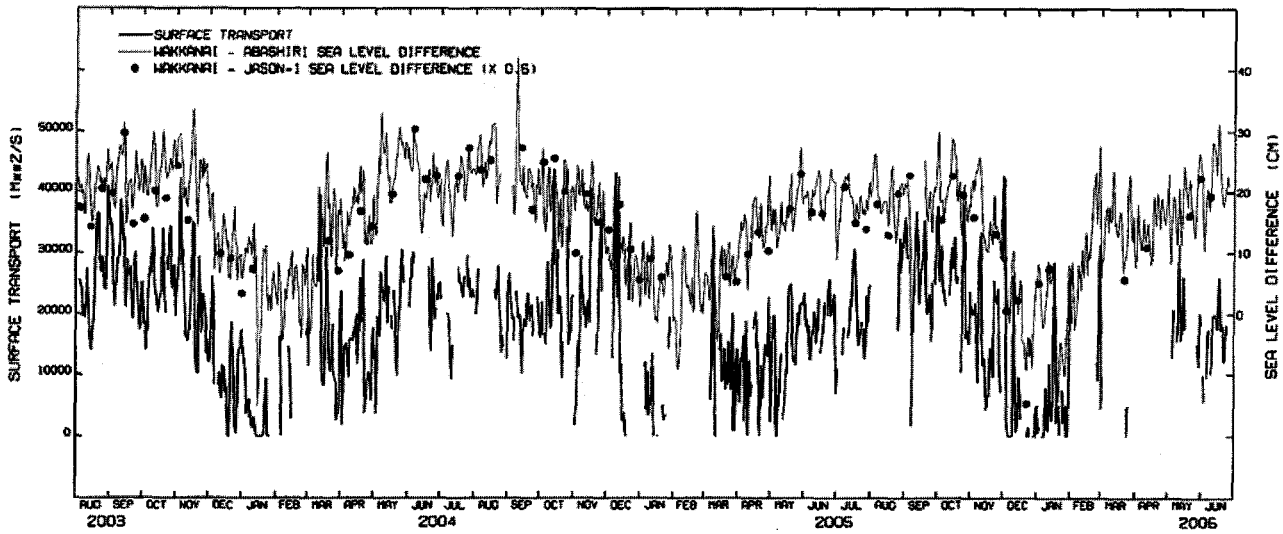

Figure 7. Time series of the surface transport of the SWC (thick line), the sea level difference between Wakkanai and Abashiri (thin line), and anomaly of the sea level difference between Wakkanai and the ground track B (Fig. 8) of the Jason-1 altimeter (solid circles).

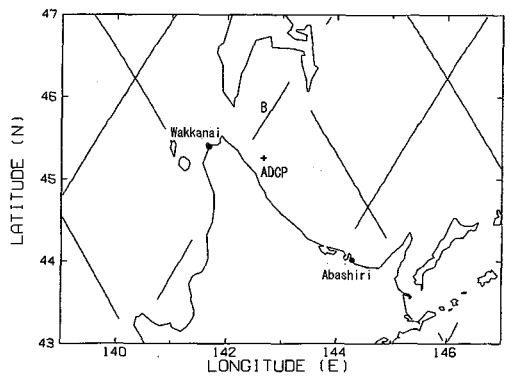

Figure 8. Locations of ground tracks of the Jason-1 altimeter and tide gauge stations of Wakkainai and Abashiri.

REFERENCES

Aota, M., 1984. Oceanographic structure of the Soya Warm Current. *Bull. Coast. Oceanogr.*, 22, pp. 30-39, (in Japanese).

Barrick, D.E., M.W. Evans, and B.L. Weber, 1977. Ocean surface currents mapped by radar. *Science*, 198, pp. 138-144.

Ebuchi, N., Y. Fukamachi, K.I. Ohshima, K. Shirasawa, M. Ishikawa, T. Takatsuka, T. Daibo, and M. Wakatsuchi, 2004. Observation of the Soya Warm Current using HF radar. *Proc. IGARSS 2004*, Anchorage, Alaska, U.S.A, September 2004, pp. 1175-1178.

Ebuchi, N., Y. Fukamachi, K.I. Ohshima, K. Shirasawa, M. Ishikawa, T. Takatsuka, T. Daibo, and M. Wakatsuchi, 2006a. Observation of the Soya Warm Current using HF radar. *J. Oceanogr.*, 62, pp. 47-61.

Ebuchi, N., Y. Fukamachi, K.I. Ohshima, K. Shirasawa, and M. Wakatsuchi, 2006b. Observation of the Soya Warm Current combining HF ocean radar with coastal tide gauges and satellite altimetry. *Proc. IGARSS 2006*, Boulder, Colorado, U.S.A, July 2006, 4 pp.

Fukamachi, Y., I. Tanaka, K.I. Ohshima, N. Ebuchi, G. Mizuta, H. Yoshida, and M. Wakatsuchi, 2006. Volume transport of the Soya Warm Current revealed by bottom-mounted ADCP and ocean-radar measurement. *Geophys. Res. Lett.* (submitted).

Matsuyama, M. Aota, I. Ogasawara, and S. Matsuyama, 1999. Seasonal variation of Soya Current. *Umi no Kenkyu*, 8, pp. 333-338 (in Japanese with English abstract and captions).

Ohshima, K.I. and M. Wakatsuchi, 1990. A numerical study of barotropic instability associated with the Soya Warm Current in the Sea of Okhotsk. J. Phys. Oceanogr., 20, pp. 570-584.

Ohshima, K.I., 1994. The flow system in the Sea of Japan caused by a sea level difference through shallow straits. J. Geophys. Res., 99, pp. 9925-9940.